Crystal Structure of Sucrose Phosphorylase from *Bifidobacterium adolescentis*†

Desiree Sprogøe,‡ Lambertus A. M. van den Broek,§ Osman Mirza,‡ Jette S. Kastrup,‡ Alphons G. J. Voragen,§ Michael Gajhede,‡ and Lars K. Skov*,‡

Structural Biology Group, Department of Medicinal Chemistry, The Danish University of Pharmaceutical Sciences, Universitetsparken 2, DK-2100 Copenhagen, Denmark, and Laboratory of Food Chemistry, Wageningen University, P.O. Box 8129, 6700 EV Wageningen, The Netherlands

Received September 11, 2003; Revised Manuscript Received November 27, 2003

ABSTRACT: Around 80 enzymes are implicated in the generic starch and sucrose pathways. One of these enzymes is sucrose phosphorylase, which reversibly catalyzes the conversion of sucrose and orthophosphate to D-Fructose and α-D-glucose 1-phosphate. Here, we present the crystal structure of sucrose phosphorylase from *Bifidobacterium adolescentis* (BiSP) refined at 1.77 Å resolution. It represents the first 3D structure of a sucrose phosphorylase and is the first structure of a phosphate-dependent enzyme from the glycoside hydrolase family 13. The structure of BiSP is composed of the four domains A, B, B′, and C. Domain A comprises the $(\beta/\alpha)_8$-barrel common to family 13. The catalytic active-site residues (Asp192 and Glu232) are located at the tips of β-sheets 4 and 5 in the $(\beta/\alpha)_8$-barrel, as required for family 13 members. The topology of the B′ domain disfavors oligosaccharide binding and reduces the size of the substrate access channel compared to other family 13 members, underlining the role of this domain in modulating the function of these enzymes. It is remarkable that the fold of the C domain is not observed in any other known hydrolases of family 13. BiSP was found as a homodimer in the crystal, and a dimer contact surface area of 960 Å^2 per monomer was calculated. The majority of the interactions are confined to the two B domains, but interactions between the loop 8 regions of the two barrels are also observed. This results in a large cavity in the dimer, including the entrance to the two active sites.

Bifidobacterium adolescentis forms one of the major groups of inhabitants of the large intestine in human adults (*1*) and can be used as a probiotic, e.g. in yogurt. Probiotics are used as microbial food supplements to beneficially affect the host by improving its intestinal microbial balance (*2*). The interaction of resistant starch with gut flora throughout the digestive tract can also promote human health (*3*). This brings the enzymes involved in starch and α-gluco-oligosaccharides (e.g. sucrose) metabolism of *B. adolescentis* in focus. Recently, two α-glucosidases from *B. adolescentis* were cloned and characterized (*4*), but to our knowledge only a single enzyme from the *Bifidobacterium* genome has been characterized by a 3D structure (*5*).

Around 80 enzymes are implicated in the generic starch and sucrose pathways according to the Kegg database (http://www.genome.ad.jp/kegg/). One of these is the sucrose phosphorylase which reversibly catalyzes the reaction

sucrose + orthophosphate = D-fructose + α-D-glucose 1-phosphate

This reaction enables the production of the essential glucose moiety from sucrose. The gene coding for sucrose phosphorylase in *B. adolescentis* (BiSP[1]) has recently been sequenced (accession no. AF543301), cloned, and characterized (*6*). BiSP consists of 504 amino acids resulting in a molecular mass of 56 189 g/mol. The only other bacterial sucrose phosphorylases purified to homogeneity and characterized today are those produced by *Pseudomonas saccharophila* (*7*), *Leuconostoc mesenteroides* (*8*, *9*), and *Streptococcus mutans* (*10*).

On the basis of amino acid sequence similarities, BiSP has been placed in the retaining glycoside hydrolase (GH) family 13 (*11*), also called the α-amylase family. Some members show transglycosidase activity, e.g. cyclomaltodextrin glucanotransferase and amylosucrase (AS). Structurally, the GH family 13 is characterized by having a $(\beta/\alpha)_8$-barrel comprising the catalytic domain and referred to as domain A. Apart from the catalytic domain, the enzymes of the family typically contain several other domains. These are named the N (N-terminal domain), B (a domain formed by the usually large loop 2 in the $(\beta/\alpha)_8$-barrel), and the C domains (C-terminal domain).

The reaction mechanism that is believed to operate in GH family 13 is a double-displacement reaction (*12*) involving a covalent glucose−enzyme intermediate. For sucrose phosphorylase from *P. saccharophila*, the existence of the intermediate was described in 1947 by Doudoroff et al. (*13*). A mechanistic scheme accommodating the synthesis of α-D-

† This work was supported by the Danish Natural Science Research Council, Apotekerfonden of 1991 and the Danish Synchrotron User Center (DANSYNC).

* Corresponding author. Telephone: +45 35306121. Fax: +45 35306040. E-mail: lsk@dfuni.dk.

‡ The Danish University of Pharmaceutical Sciences.

§ Wageningen University.

[1] Abbreviations: AS, amylosucrase; BiSP, sucrose phosphorylase from *Bifidobacterium adolescentis*; GH, glycosyl hydrolase; rms, root-mean-square.

10.1021/bi0356395 CCC: $27.50
Published on Web 01/16/2004

Scheme 1. Sucrose Phosphorylase Reaction Mechanism

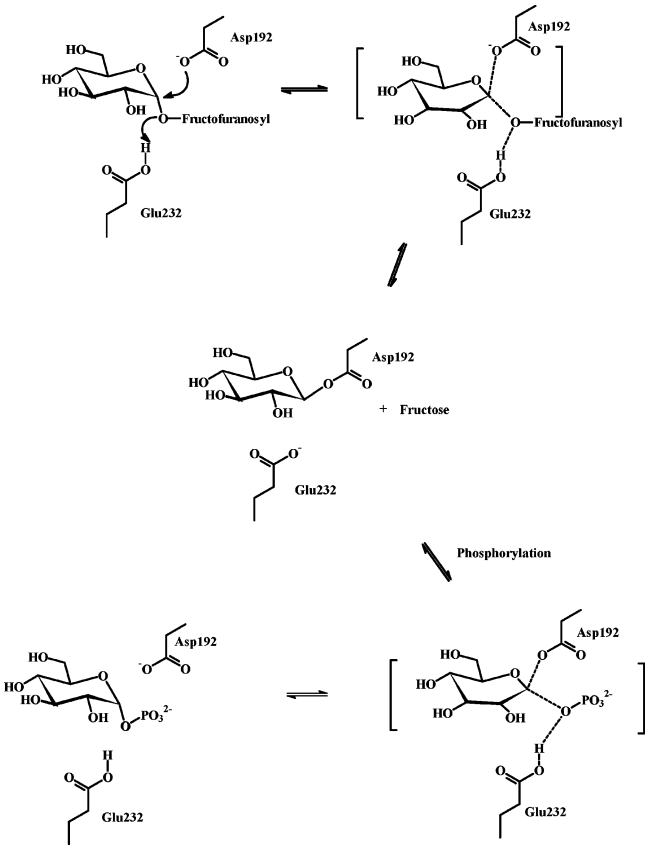

glucose 1-phosphate from sucrose and inorganic phosphate is shown in Scheme 1. The reaction is initiated by simultaneous protonation of the sucrose glycosidic bond by the proton donor (identified as Glu232) and a nucleophilic attack by Asp192 on the anomeric carbon of the glucose moiety. This leads to the covalently linked substrate−enzyme intermediate and the release of fructose. The intermediate can then react with phosphate (HPO_4^{2-} or $H_2PO_4^-$), and finally glucose 1-phosphate is released. Reaction with other nucleophiles such as water or saccharides is also possible. A detailed kinetic study of BiSP has not been performed yet, but sucrose phosphorylase from *P. saccharophila* has been thoroughly examined previously (*7*). For this enzyme, the initial rate of sucrose consumption was 56 times higher for phosphate than for water. It was also found that glucose, fructose, and phosphate could inhibit the enzyme and that the affinity for glucose was about 500 times greater than that for fructose or phosphate.

In this paper, we present the crystal structure of BiSP refined at a resolution of 1.77 Å. It represents the first crystal structure of a sucrose phosphorylase and is the first structure of a phosphate-dependent enzyme from the GH family 13. This detailed structural investigation of a sucrose phosphorylase has increased our understanding of the basis of substrate specificity and will be an important tool for further engineering of enzymes involved in the starch and sucrose metabolism.

EXPERIMENTAL PROCEDURES

Crystallization and Data Collection. Recombinant protein expression and purification from cell free extract of *B. adolescentis* DSM20083 is described separately (*6*). Crystallization conditions were screened according to the sparse-matrix method (*14*) using commercially available buffers (Hampton Research, Laguna Hills, CA) and the hanging-drop vapor-diffusion technique (*15*). Hanging drops were prepared by mixing 2.5 μL of protein solution (0.5−1.0 mg/mL, 10 mM Tris/HCl pH 7.1) with 2.5 μL of precipitant solution (27 w/v % poly(ethylene glycol)4000, 0.1 M Tris/HCl pH 8.5, and 0.1 M sodium acetate) and equilibrated against 500 μL of precipitant at 25 °C. Crystals grew within 3−14 days. All crystals were flash-cooled in liquid nitrogen prior to data collection. A native data set was collected to 1.8 Å resolution at 120 K on an in-house MAR345 image plate detector using Cu Kα radiation. A second native data set to 1.58 Å was collected at PSF, BESSY, Berlin, Germany, on a MARCCD.

For phase determination, a $Hg(CH_3CO_2)_2$ derivative was prepared. $Hg(CH_3CO_2)_2$ was dissolved in 1 mL of precipitant, and 0.3 μL was added to the hanging drops with crystals. Crystals were soaked for 8 days and brought to beamline 711, MAXLABII Synchrotron Facility, Lund, Sweden. A 2.05 Å SAD data set was collected at 110 K on a MARCCD.

Data from MAXLABII and in-house were processed with Denzo and Scalepack (*16*), whereas native data from BESSY were processed with Mosflm (*17*) and Scala (*18*). All crystals belong to the orthorhombic space group $P2_12_12_1$, with two molecules in the asymmetric unit and with approximately the same cell dimensions: $a = 55.04$, $b = 123.35$, and $c = 151.48$ Å (from high-resolution BESSY data).

Structure Determination and Refinement. SIRAS phases were calculated on the basis of the heavy atom derivative $Hg(CH_3CO_2)_2$. The heavy atom positions were identified from peaks in the anomalous and isomorphous difference Patterson maps using the CCP4 program suite (*18*). Heavy atom positions were refined and the phases calculated with the program Sharp (*19*), followed by solvent density modification with a solvent content of 45.2% by the CCP4 program Solomon (*20*). The resulting electron density map was easily traced using the program Arp/Warp (*21*) with data to 1.58 Å resolution, although $I/\sigma I$ was quite low below 1.77 Å. The model was refined with CNS (*22*) with the mlf target function against data from 20.0 to 1.77 Å using a bulk solvent model and anisotropic *B*-factor correction. Refinement steps were accepted if they produced a lowering of R_{free}. Water molecules were picked among spherical peaks of 1.2σ in the $2F_o - F_c$ maps and were analyzed for hydrogen-bonding interaction with the protein or other water molecules. The temperature factors were refined for every atom but restrained to the temperature factors of neighboring atoms. The data and refinement statistics are listed in Table 1. Two BiSP molecules (A and B) resulting in a total of 1008 amino acid residues, two Tris ions, and 1412 water molecules were included in the final model. Sixteen of the side chains were fitted with two conformations, and for 17 surface side chains some of the outermost atoms displayed high *B*-factors (>40 Å^2).

The Ramachandran plot as calculated by the program PROCHECK (*23*) shows 89.9% of the residues in the most favorable regions, 9.6% in the additional allowed regions, 0.6% (Phe156 and Asp446 in both molecules and Asp447 in molecule B) in the generously allowed regions, and no residues in disallowed regions of the plot. The atomic coordinates as well as structure factors of BiSP have been

Table 1. Crystallographic Data and Model Refinement

Data Collection and Analysis

	native (in house)	$Hg(CH_3CO_2)_2$	native (Bessy)
resolution range, Å (outer shell)	20.0−2.00 (2.07−2.00)	51.9−2.04 (2.15−2.04)	23.3−1.58 (1.66−1.58)
wavelength, Å	1.542	0.996	0.918
completeness, % (outer shell)	87.9 (88.6)	99.4 (99.4)	97.8 (85.2)
redundancy (outer shell)	3.4 (3.0)	9.2 (8.6)	3.7 (3.2)
R_{sym},[a] % (outer shell)	12.9 (32.9)	8.24 (23.5)	10.9 (53)
$I/\sigma I$ (outer shell)	9.1 (3.3)	8.2 (3.2)	4.3 (0.9)

Heavy Atom Refinement

no. of Hg sites		6	
resolution range, Å		51.9−2.04	51.9−3.41
phasing power,[b] isomorphous acentric/centric		0.64/0.53	0.9/0.7
phasing power,[b] anomalous		0.61	1.50
R_{cullis},[c] isomorphous acentric/centric		0.84/0.83	0.82/0.80
R_{cullis},[c] anomalous		0.93	0.71
FOM[d] after SHARP acentric/centric		0.25/0.20	0.52/0.32
FOM[d] after Solomon		0.84	

Refinement Statistics

no. of reflections (free)	resolution, Å	R_{conv}[e]/R_{free},[f] %	no. of non-H protein/water/Tris atoms	rmsd bonds, Å	rmsd angles, deg
101 196 (5 198)	20.0−1.77	15.8/19.1	7 912/1 412/16	0.006	1.4

[a] $R_{sym} = \sum_{hkl}(\sum_i(|I_{hkl,i} - \langle I_{hkl}\rangle|))/\sum_{hkl,i}\langle I_{hkl}\rangle$, where $I_{hkl,i}$ is the intensity of an individual measurement of the reflection with Miller indicies h, k, and l, and $\langle I_{hkl}\rangle$ is the mean intensity of that reflection. [b] Phasing power $= \sum_{hkl}F_{H,hkl}/\sum_{hkl}|F_{PH,obs,hkl} - F_{PH,calc,hkl}|$. [c] $R_{cullis} = \sum_{hkl}||F_{PH,hkl} \pm F_{P,hkl}| - F_{H,calc,hkl}|/\sum_{hkl}|F_{PH,hkl} - F_{P,hkl}|$, where F_{PH} is the structure factor of the heavy atom derivative, F_P is the structure factor of the native protein, and $F_{H,calc}$ is the calculated structure factor for the heavy atom. [d] Figure of merit. [e] $R_{conv} = \sum_{hkl}(||F_{obs,hkl}| - |F_{calc,hkl}||)/|F_{obs,hkl}|$, where $|F_{obs,\ hkl}|$ and $|F_{calc,hkl}|$ are the observed and calculated structure factor amplitudes. [f] R_{free} is equivalent to the R_{conv}, but calculated with 5% of the reflections omitted from the refinement process.

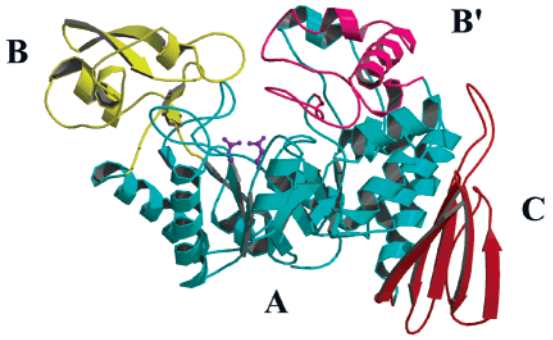

FIGURE 1: Richardson representation of the monomer structure of BiSP (molecule A). Domain A is displayed in blue, domain B in yellow, domain B′ in magenta, and domain C in red. The catalytic active residues (Asp192 and Glu232) are shown in purple.

deposited in the Protein Data Bank (PDB) with the accession code 1R7A.

RESULTS AND DISCUSSION

Fold Description. Two BiSP molecules (A and B) are found in the asymmetric unit of the crystal. The fold is identical for both polypeptide chains, and the structures can be superimposed with an rms deviation of 0.25 Å on 504 Cα atoms. The single polypeptide chain is folded into a structure with four domains, named A, B, B′, and C (Figure 1).

Domain A (residues 1−85, 167−291, and 356−435) is made up of eight alternating parallel β-strands (e1−e8) and α-helices (h1−h8), giving a $(\beta/\alpha)_8$-barrel common to the GH family 13. A characteristic of the $(\beta/\alpha)_8$-barrel enzymes is that the loops connecting strands to helices are much longer on average than those connecting helices to strands. BiSP has two long loops (81 amino acid residues in the loop between e3 and h3, and 64 amino acid residues in the loop between e7 and h7) displaying structural elements, and we have classified them as separate domains B and B′, respectively. Domain B (residues 86−166) contains two short antiparallel β-sheets and two short α-helices. The inner sheet (relative to the barrel) is formed by two strands (residues 88−90 and 160−162), and the outer sheet is formed by two strands (residues 140−145 and 148−153), flanked by the two α-helices (residues 94−102 and 125−129). Domain B′ (residues 292−355) is mainly a coil region but contains one long α-helix (residues 312−325) and a short α-helix (residues 330−337).

Although the complete BiSP sequence contains two cysteine residues, no disulfide bridges are found in the structure. One of the cysteines (Cys356) is exposed on the surface and is in this structure (with data generated by synchrotron radiation) oxidized to a sulfone, making it a modified amino acid (Csw356). However, in the structure generated by our in-house source, it is still a cysteine. The other cysteine (Cys205) is located in the interior of the enzyme.

The 56 first residues of the C-terminal domain (Figure 1) form a single five-stranded antiparallel β-sheet with a topology described as 1,1,1,1 in algebraic notation. After a turn, the last six residues are below this sheet and are found in an extended conformation. Strands 1−3 are connected by short hairpin loops, whereas the loop between strands 3 and 4 is formed by 16 residues. The tip of the loop is in proximity of the B′ domain and actually blocks some of the regions equivalent to oligosaccharide binding site OB2 in the amylosucrase structure (*24*). This probably makes the domain partially responsible for the change in substrate specificity between the two closely related enzymes.

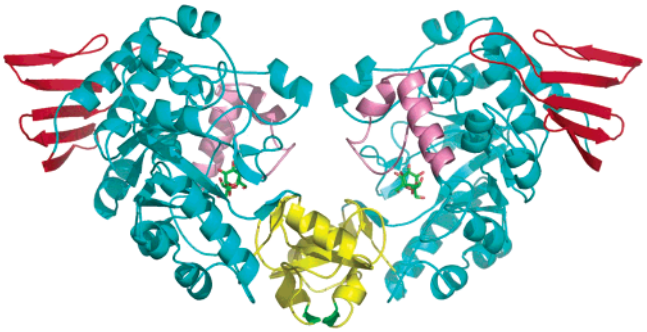

FIGURE 2: Richardson representation of the homodimer (molecule A and B) of BiSP. The noncrystallographic two-fold symmetry axis is approximately vertical. The color coding is identical to Figure 1. The majority of the interactions are confined to the two B domains shown in yellow, and the β-sheet type backbone interactions formed between the two domains are colored green. Sucrose molecules have been modeled into the active sites on the basis of superposition of the structures of BiSP and an AS:sucrose complex.

It is remarkable that the fold of the C domain is not observed in any of the other known hydrolases in GH family 13. The fold of the β-sandwich domain observed in many of the family 13 hydrolases can, however, be derived from the BiSP fold. Loop 3 in e.g. AS is even longer than that in BiSP and forms the second sheet of the β-sandwich. The sandwich domains terminate after a strand that coincides with BiSP strand 4. These relations reflect the common origin the hydrolases of GH family 13. A DALI search (*25*) with the C domain alone revealed that the FhuA receptor (PDB accession no. 1BY5) (*26*) displays the highest similarity (*Z* score 5.1). However, the aligned regions were only parts of the very long strands forming the transmembrane pore of FhuA. A corresponding region of the sucrose specific porin (1A0T) (*27*) was also found to be similar (*Z* score 5.1) to the C domain. This suggests that the domain has a very unusual fold, and also that this domain conformation is highly dependent on interactions with the $(\beta/\alpha)_8$ barrel.

Dimer Formation. Native molecular weight determination indicated that BiSP is a homodimer in solution, estimated by gel filtration experiments at pH 6.5 (*6*). To verify the dimer formation at crystallization pH, dynamic light scat-

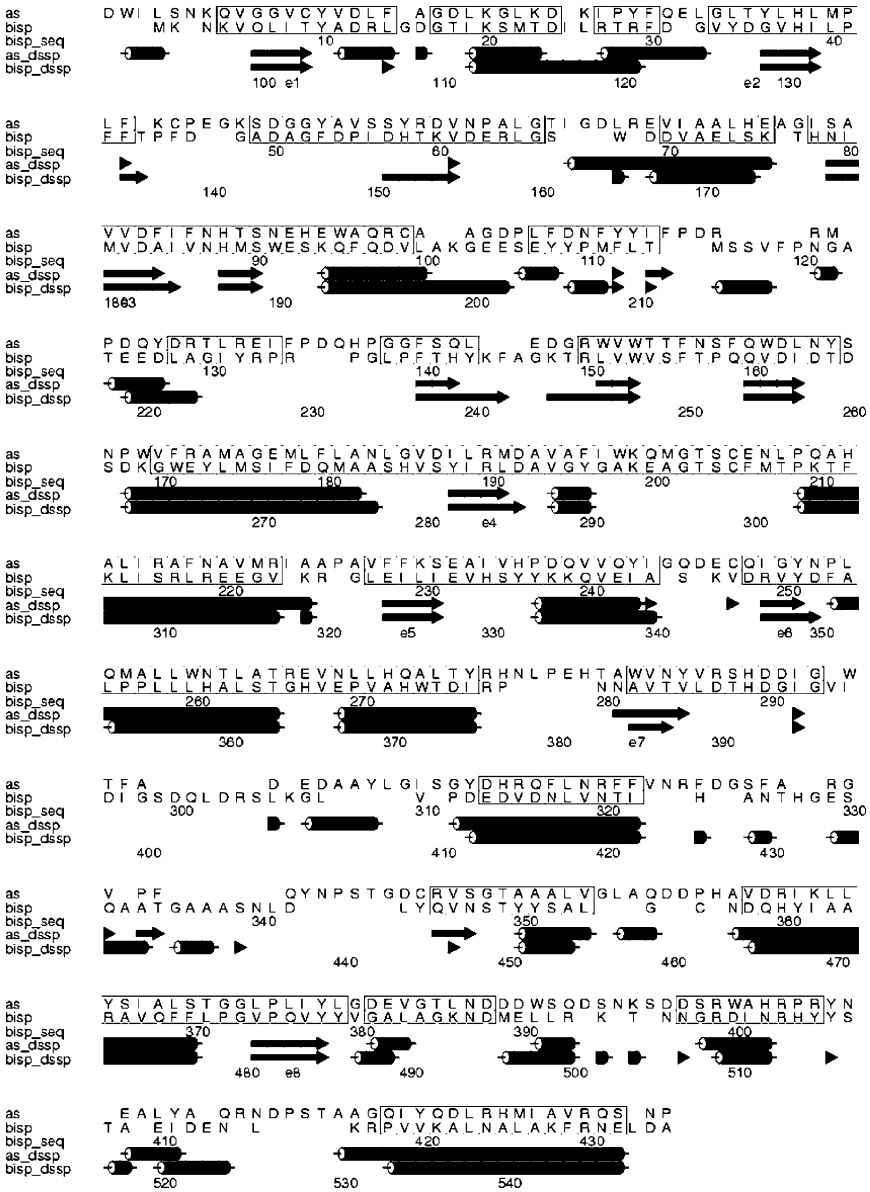

FIGURE 3: Structural alignment (*41*, *42*) of BiSP and the structurally related enzyme amylosucrase (AS) using the Kabsch−Sander algorithm (*43*).

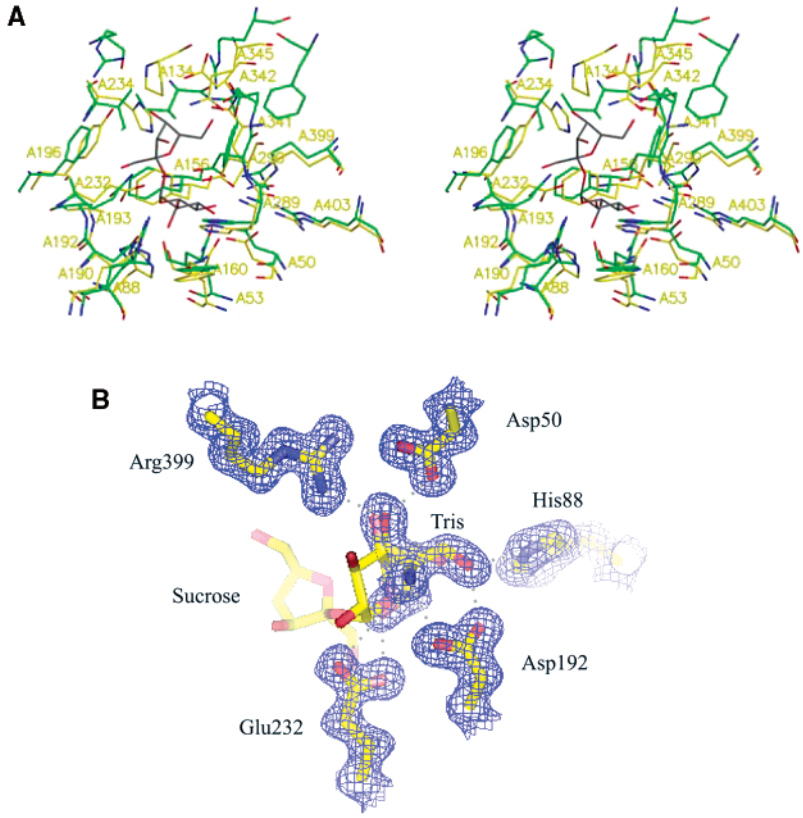

FIGURE 4: Active site of BiSP. (A) Superposition of the active site residues of BiSP (in green) and AS (in yellow). The sucrose molecule of the AS:sucrose complex is shown in black. Heteroatoms are in standard colors: nitrogen atoms are blue and oxygen atoms red. (B) Zoom on the Tris molecule observed in the active site of BiSP. The final $2F_o - F_c$ electron density contoured at 1σ is shown in blue. Hydrogen bonds are displayed as dotted lines.

tering was performed. Results confirmed dimer formation at crystallization pH 8.5 and at pH 6.5 (data not shown).

The symmetry of the crystal gave a number of possible dimers, which were submitted to the Protein−Protein Interaction Server (*28*). This analysis showed that two likely dimers could be identified. Dimer 1 had a dimer interface area of 960 Å^2 (per monomer), while the area in dimer 2 was 910 Å^2. The total surface area of a monomer is 21,400 Å^2. Since both dimer interfaces are of significant size, direct hydrogen bonds and water-mediated hydrogen bonds were analyzed using PyMOL (DeLano Scientific LLC, San Carlos, CA) and the CCP4 program Contact. The dimer 1 interface contains 11 hydrogen bonds, two salt bridges, and five bridging water molecules. The dimer 2 interface is built of four hydrogen bonds, no salt bridges, and eight bridging water molecules out of a large number of other water molecules located at the interface. The intermolecular forces in dimer 1 appear much stronger than those in dimer 2. In addition, β-sheet-type backbone interactions are formed across dimer 1. Therefore, we conclude that dimer 1 is the most likely solution dimer.

The suggested BiSP dimer is depicted in Figure 2. The majority of the interactions are confined to the two B domains, but interactions between the loop 8 regions of the two barrels are also observed. This results in a large cavity in the dimer, which includes the entrance to the two active sites. Other known structures of dimers in the GH family 13 are formed by the enzymes cyclomaltodextrinase (*29*), neopullulanase (*30*), and maltogenic amylase (*31*). In contrast to the BiSP dimer, the other dimers were primarily formed by the hydrolase N-terminal domains. To our knowledge, the BiSP structure represents the first assignment of a functional role of a B domain for dimerization in the entire GH family 13.

Active Site. In a BLAST search with known 3D structure, the highest alignment score for BiSP was obtained with AS (*32*). The aligned regions cover the first half of the $(\beta/\alpha)_8$-barrel of AS (Figure 3). A pairwise alignment of the two sequences using the Clustal W algorithm (*33*) also aligned the sequences after the unique amylosucrase N-terminal domain. The alignment covered the whole AS catalytic and C-terminal domain. Furthermore, the Pfam alignment server (*34*) identifies a full amylase domain ($(\beta/\alpha)_8$-barrel and C-terminal sandwich domain) in BiSP. This alignment shows that a B′ domain is present, as is the case for AS (*35*). The B′ domain is formed by loop 7 of the $(\beta/\alpha)_8$-barrel and comprises 64 residues, as compared to 55 in AS. The loop is exceptionally long in BiSP and AS as compared to the hydrolases of GH family 13 in general and probably explains the high BLAST alignment score against AS. In AS, this loop contains two oligosaccharide binding sites, referred to as OB1, which includes the binding sites −1 to +5 of the hydrolases in GH family 13, and the high-affinity binding site OB2 somewhat distant from the active site (*24*). Hence, it has been suggested that this domain is largely responsible for the polymerase properties.

A DALI search (*25*) with the whole BiSP molecule clearly revealed AS as the protein with the highest similarity score, demonstrating that structural alignment of BiSP and AS: substrate complexes is well suited as a basis for understanding the product profile and substrate specificity observed of BiSP. The BiSP active site was easily identified by super-

imposing the structures of BiSP and AS. The superimposed active site region of BiSP and of the AS:sucrose complex is shown in Figure 4A. The active site of AS has previously been compared to active sites of the hydrolases of family 13, and a high degree of similarity has been established (*35*). Thus, the AS active site can be regarded as representative for the entire family 13. The nucleophilic aspartates and the general acid/base glutamates (glutamine in the inactivated AS:sucrose complex) are seen to superimpose very well. Asp192 and Glu232 are found at the tips of β-sheets 4 and 5 in the $(\beta/\alpha)_8$-barrel of the enzyme, as required for family 13 members. The distance between Asp192 Cα and Glu232 Cα is 5.5 Å, in accordance with BiSP being an α-retaining enzyme (*36*). The third carboxylate conserved in the active site of family 13 enzymes is also found here (Asp290) and can be seen in Figure 4A. A Tris molecule is bound at the active site of BiSP (Figure 4B), forming a short hydrogen bond from an oxygen atom to Oδ2 of Asp192 (2.6 Å) and in addition several hydrogen bonds to surrounding amino acid side chains (Asp50, His88, Glu232, and Arg399). In Figure 4B, it can be seen that Tris occupies several of the sucrose binding positions (based on a superimposition between BiSP and the AS:sucrose complex), and this probably explains why it has previously been found in the active site of a number of structures of α-amylases (*37*).

The residues involved in the binding of the glucosyl moiety (in amylase nomenclature corresponding to subsite -1 interactions (*38*)) are structurally conserved. The BiSP active site can accommodate the sucrose molecule without a need for major structural rearrangements, even though the fructosyl moiety surroundings are much less conserved as compared to the glucosyl binding site. Here, only Tyr196 is found in a position that is occupied by an aromatic residue in AS. No calcium ions were found in the structure, as probably expected of a phosphate-dependent enzyme. In BiSP, a lysine Nζ (Lys199) is positioned at the site normally occupying the calcium ion in other family 13 enzymes. Several features of this calcium site are structurally conserved, as also found in AS (*35*) and oligo-1,6-glucosidase (*39*).

After the formation of the covalent intermediate, a phosphate ion must enter the active site (Scheme 1). For steric reasons, the phosphate ion must bind at the position previously occupied by the fructosyl moiety, or at least very close to this position. Thus, one would expect a relatively positive electrostatic potential in this region. Several remarkable changes are observed between BiSP and AS. At the position of AS Ile330, a histidine residue (His234) was found in BiSP. This change introduces a positive charge in the active site, at least at acidic pH. In any case, the histidine residue is also positioned ideally for hydrogen bond formation to the phosphate ion, and we expect a phosphate ion to bind here. This is also supported by the presence of Gln345 at an AS aspartate position. Another change is perhaps more surprising. In BiSP, Asp342 now occupies an AS arginine position and probably contributes to a less positive electrostatic potential. These latter findings could indicate that structural rearrangements are involved at some stage of the reaction mechanism.

Substrate Access Channel. In Figure 5A, the structures of BiSP and AS are viewed down the active site access channel, with the sucrose molecule of the AS structure included (*40*). The BiSP channel appears much smaller than that of AS. A loop from the B′ domain seems to be largely responsible for reduced size, and this observation again stresses the importance of the B′ domain and its role in modulating the function of family 13 enzymes. In BiSP, the topology of the B′ domain disfavors oligosaccharide binding and reduces the size of the substrate access channel, whereas in the polymerase AS the B′ domain topology is essential for oligosaccharide binding. Hydrolases such as amylases have no B′ domain, and this results in a cleft-like active site topology. As shown in Figure 5B, the BiSP dimer formation does not block the access to the active sites of the dimer.

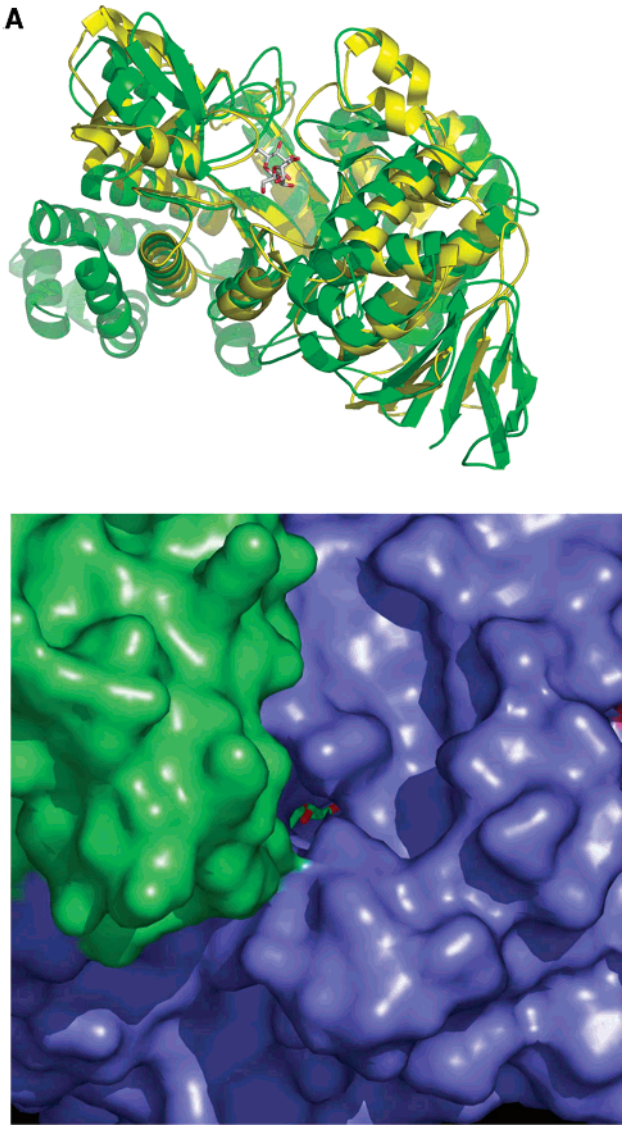

FIGURE 5: Substrate access channel. (A) An aligned cartoon representation of BiSP (in green) and AS (in yellow) viewed down the substrate access channel, with the sucrose molecule of AS included in stick representation. (B) PyMOL picture of a close-up of the solvent accessible surface representation of the BiSP homodimer (molecules A and B) including the sucrose molecule from the AS:sucrose complex. The surfaces of molecules A and B are colored in blue and green, respectively.

BiSP catalyzes a reaction with a smaller secondary substrate than AS and can consequently function with a smaller active site access channel. However, one basic problem is the same, namely the protection of the covalent intermediate against hydrolysis. AS probably solves this problem by having oligosaccharides block the substrate access channel

after fructose release (*24*). How this problem is solved in BiSP will have to await structure determinations of intermediates in the reaction cycle.

ACKNOWLEDGMENT

We acknowledge MAX-LABII and the staff at beamline 711 and the Protein Factory, BESSY, for provision of synchrotron radiation facilities.

REFERENCES

1. Matsuki, T., Watanabe, K., Tanaka, R., Fukuda, M., and Oyaizu, H. (1999) *Appl. Environ. Microbiol. 65*, 4506−4512.
2. Gibson, G. R., and Roberfroid, M. B. (1995) *J. Nutr. 125*, 1401−1412.
3. Bird, A. R., Brown, I. L., and Topping, D. L. (2000) *Curr. Issues Intest. Microbiol. 1*, 25−37.
4. van den Broek, L. A. M., Struijs, K., Verdoes, J. C., Beldman, G., and Voragen, A. G. J. (2003) *Appl. Microbiol. Biotechnol. 61*, 55−60.
5. Iwata, S., and Ohta, T. (1993) *J. Mol. Biol. 230*, 21−27.
6. van den Broek, L. A. M., van Boxtel, E. L., Kievit, R. P., Verhoef, R., Beldman, G., and Voragen, A. G. J. *Appl. Microbiol. Biotechnol.*, in press (DOI: 10.1007/s00253-003-1534-x).
7. Silverstein, R., Voet, J., Reed, D., and Abeles, R. H. (1967) *J. Biol. Chem. 242*, 1338−1346.
8. Koga, T., Nakamura, K., Shirokane, Y., Mizusawa, K., Kitao, S., and Kikuchi, M. (1991) *Agric. Biol. Chem. 55*, 1805−1810.
9. Kawasaki, H., Nakamura, N., Ohmori, M., Amari, K., and Sakai, T. (1996) *Biosci., Biotechnol., Biochem. 60*, 319−321.
10. Russell, R. R. B., Mukasa, H., Shimamura, A., and Ferretti, J. J. (1988) *Infect. Immun. 56*, 2763−2765.
11. Coutinho, P. M., and Henrissat, B. (1999) http://afmb.cnrs-mrs.fr/~pedro/CAZY.
12. Koshland, D. E. (1953) *Biol. Rev. Camb. Philos. Soc. 28*, 416−436.
13. Doudoroff, M., Barker, H. A., and Hassid, W. Z. (1947) *J. Biol. Chem. 168*, 725−732.
14. Jancarik, J., and Kim, S. H. (1991) *J. Appl. Crystallogr. 24*, 409−411.
15. Mcpherson, A. (1992) *J. Cryst. Growth 122*, 161−167.
16. Otwinowski, Z., and Minor, W. (1997) *Macromol. Cryst., Pt. A 276*, 307−326.
17. Leslie, A. G. W. (1992) *Joint CCP4 and ESF-EACMB Newsletter on Protein Crystallography 26*, SERC Daresbury Laboratory, Warrington, U.K.
18. Bailey, S. (1994) *Acta Crystallogr. D50*, 760−763.
19. de La Fortelle, E., and Bricogne, G. (1997) *Methods Enzymol. 276*, 472−494.
20. Abrahams, J. P., and Leslie, A. G. W. (1996) *Acta Crystallogr. D52*, 30−42.
21. Perrakis, A., Morris, R., and Lamzin, V. S. (1999) *Nat. Struct. Biol. 6*, 458−463.
22. Brunger, A. T., Adams, P. D., Clore, G. M., DeLano, W. L., Gros, P., Grosse-Kunstleve, R. W., Jiang, J. S., Kuszewski, J., Nilges, M., Pannu, N. S., Read, R. J., Rice, L. M., Simonson, T., and Warren, G. L. (1998) *Acta Crystallogr. D54*, 905−921.
23. Laskowski, R. A., Macarthur, M. W., Moss, D. S., and Thornton, J. M. (1993) *J. Appl. Crystallogr. 26*, 283−291.
24. Skov, L. K., Mirza, O., Sprogøe, D., Dar, I., Remaud-Simeon, M., Albenne, C., Monsan, P., and Gajhede, M. (2002) *J. Biol. Chem. 277*, 47741−47747.
25. Holm, L., and Sander, C. (1995) *Trends Biochem. Sci. 20*, 478−480.
26. Locher, K. P., Rees, B., Koebnik, R., Mitschler, A., Moulinier, L., Rosenbusch, J. P., and Moras, D. (1998) *Cell 95*, 771−778.
27. Forst, D., Welte, W., Wacker, T., and Diederichs, K. (1998) *Nat. Struct. Biol. 5*, 37−46.
28. Jones, S., and Thornton, J. M. (1996) *Proc. Natl. Acad. Sci. U.S.A. 93*, 13−20.
29. Lee, H. S., Kim, M. S., Cho, H. S., Kim, J. I., Kim, T. J., Choi, J. H., Park, C., Lee, H. S., Oh, B. H., and Park, K. H. (2002) *J. Biol. Chem. 277*, 21891−21897.
30. Hondoh, H., Kuriki, T., and Matsuura, Y. (2003) *J. Mol. Biol. 326*, 177−188.
31. Kim, J. S., Cha, S. S., Kim, H. J., Kim, T. J., Ha, N. C., Oh, S. T., Cho, H. S., Cho, M. J., Kim, M. J., Lee, H. S., Kim, J. W., Choi, K. Y., Park, K. H., and Oh, B. H. (1999) *J. Biol. Chem. 274*, 26279−26286.
32. De Montalk, G. P., Remaud-Simeon, M., Willemot, R. M., Planchot, V., and Monsan, P. (1999) *J. Bacteriol. 181*, 375−381.
33. Thompson, J. D., Higgins, D. G., and Gibson, T. J. (1994) *Nucleic Acids Res. 22*, 4673−4680.
34. Bateman, A., Birney, E., Durbin, R., Eddy, S. R., Finn, R. D., and Sonnhammer, E. L. L. (1999) *Nucleic Acids Res. 27*, 260−262.
35. Skov, L. K., Mirza, O., Henriksen, A., De Montalk, G. P., Remaud-Simeon, M., Sarcabal, P., Willemot, R. M., Monsan, P., and Gajhede, M. (2001) *J. Biol. Chem. 276*, 25273−25278.
36. Davies, G., and Henrissat, B. (1995) *Structure 3*, 853−859.
37. Aghajari, N., Feller, G., Gerday, C., and Haser, R. (1998) *Protein Sci. 7*, 564−572.
38. Davies, G. J., Wilson, K. S., and Henrissat, B. (1997) *Biochem. J. 321*, 557−559.
39. Watanabe, K., Hata, Y., Kizaki, H., Katsube, Y., and Suzuki, Y. (1997) *J. Mol. Biol. 269*, 142−153.
40. Mirza, O., Skov, L. K., Remaud-Simeon, M., De Montalk, G. P., Albenne, C., Monsan, P., and Gajhede, M. (2001) *Biochemistry 40*, 9032−9039.
41. Russell, R. B., and Barton, G. J. (1992) *Proteins 14*, 309−323.
42. Barton, G. J. (1993) *Protein Eng. 6*, 37−40.
43. Kabsch, W., and Sander, C. (1983) *Biopolymers 22*, 2577−2637.

BI0356395